

# Metal-Catalyzed Hydrocarbon Conversion Reactions<sup>†</sup>

W. T. Tysoe\*

Department of Chemistry and Laboratory for Surface Studies,  
University of Wisconsin–Milwaukee, Milwaukee, Wisconsin 53211

Received September 1, 1994<sup>Ⓢ</sup>

Palladium-catalyzed acetylene trimerization and the metathesis of olefins catalyzed by molybdenum and its oxides are investigated in ultrahigh vacuum and at high pressures. Benzene is formed on Pd(111) by the reaction between adsorbed acetylene and a surface C<sub>4</sub> metallocycle. The resulting benzene evolves in temperature-programmed desorption in two distinct states. The low-temperature state is proposed, following investigations of the desorption kinetics of benzene from Pd(111), to be due to tilted benzene formed on a sterically crowded surface, and the high-temperature state, to be due to flat-lying benzene. The low steady-state benzene formation rate found at high pressures (~1 atm) is suggested to be due to blocking of the surface by the formation of vinylidene species. Olefin metathesis is found to proceed in two different regimes: one below ~650 K, which mimics supported molybdena catalysts and where MoO<sub>3</sub> is the best catalyst, and another region above this temperature, where the reaction proceeds with a high activation energy (~60 kcal/mol) and the most effective catalyst is MoO<sub>2</sub>. The latter kinetics resemble those found for metallic molybdenum, where the reaction is proposed to proceed by a mechanism through which alkenes dissociate and recombine on the surface. This reaction is found to proceed in the presence of a thick carbonaceous layer. The addition of hydrogen is found to increase the rate of both metathesis and cyclotrimerization even though neither of these reactions involves hydrogen directly. This is proposed to be due to the titration of carbonaceous species from the surface. Extension of these ideas to ethylene hydrogenation, a reaction that *does* involve hydrogen, is successful in rationalizing the kinetics behavior found in that case.

## 1. Introduction

Transition metals and their oxides are capable of catalyzing a range of hydrocarbon conversion reactions, and examples of these include the metathesis of olefins and acetylene cyclotrimerization. The former reaction is conventionally catalyzed by oxides of molybdenum,<sup>1,2</sup> although it is shown that metallic molybdenum is also capable of catalyzing the reaction at sufficiently high temperatures.<sup>3</sup> Acetylene cyclotrimerization is catalyzed by metallic palladium<sup>4,5</sup> and is relatively unique to this metal although other transition metals, for example, nickel<sup>6</sup> and copper<sup>7</sup> as well as tin-modified platinum,<sup>8</sup> are also capable of catalyzing the reaction.

The experimental strategy used to scrutinize the reaction pathway is to examine the chemistry of the reactants on model catalysts using the wide range of surface-sensitive techniques that are now available and comparing this chemistry with that found at high pressures (several Torr) using the same model catalyst. These experiments are most conveniently carried out by incorporating a high-pressure reactor directly into the ultrahigh vacuum chamber, which allows surface science and catalytic experiments to be carried out on the same sample.<sup>9,10</sup> This further allows the kinetics of the model system to be compared with the commercial catalyst to

establish how well the model reproduces the “real world” system. Palladium-catalyzed acetylene cyclotrimerization presents a rather unique reaction for implementing this type of strategy because benzene is formed from acetylene both at low pressures (following acetylene adsorption on a single-crystal surface in ultrahigh vacuum)<sup>5</sup> and at high pressures using this sample.<sup>11</sup> This allows the benzene formation pathway on Pd(111) to be probed in some detail.

However, it is often found that reactions observed at high pressure do not proceed similarly in ultrahigh vacuum. The molybdenum and molybdenum oxide catalyzed metathesis of olefins exemplifies this situation rather well although, even in these cases, detailed studies of the surface chemistry of the reactants can provide important insights into the catalytic reaction pathway.<sup>12</sup> For example, it is shown that, at high reaction temperatures (> 650 K), metathesis proceeds via a dissociative/associative mechanism. This reaction illustrates another important advantage of including a catalytic reaction cell directly into an ultrahigh vacuum chamber: the possibility of being able to chemically modify the catalyst in a controlled manner, characterize the catalyst, and transfer it directly into the reaction cell without any intervening exposure to air. The most effective olefin metathesis catalyst consists of a supported oxide of molybdenum which is then calcined to form an intermediate oxidation state. Various oxidation states of molybdenum can be prepared, under controlled conditions, either in the ultrahigh vacuum portion of the apparatus or, more vigorously, in the high-pressure cell, and the resulting activity of the catalyst can be measured. This type of experiment shows that MoO<sub>2</sub> and MoO<sub>3</sub> appear to provide the most effective metathesis catalyst, depending on the reaction temperature.<sup>13</sup>

\* Author to whom correspondence should be addressed. Telephone: (414) 229-5222. FAX: (414) 229-5530. E-mail: WTT@ALPHA2.CSD.UWM.EDU.

<sup>†</sup> Paper presented at the symposium on Advances in the Measurement and Modeling of Surface Phenomena, San Luis, Argentina.

<sup>Ⓢ</sup> Abstract published in *Advance ACS Abstracts*, January 1, 1996.

(1) Banks, R. L.; Bailey, G. C. *Ind. Eng. Chem. Prod. Res. Dev.* **1964**, *3*, 170.

(2) Bowman, R. G.; Burwell, R. L., Jr. *J. Catal.* **1984**, *88*, 388.

(3) Wang, L. P.; Soto, C.; Tysoe, W. T. *J. Catal.* **1993**, *143*, 92.

(4) Berthelot, M. *Justus Liebig's Ann. Chem.* **1967**, *141*, 173.

(5) Tysoe, W. T.; Nyberg, G. L.; Lambert, R. M. *J. Chem. Soc., Chem. Commun.* **1990**, 1421.

(6) Bertolini, J. C.; Massardier, J.; Dalmay-Imelik, G. *J. Chem. Soc., Faraday Trans. 1* **1978**, 1720.

(7) Avery, N. R. *J. Am. Chem. Soc.* **1985**, *107*, 6711.

(8) Xu, C.; Peck, J. W.; Koel, B. E. *J. Am. Chem. Soc.* **1993**, *115*, 751.

(9) Wang, L. P.; Tysoe, W. T. *J. Catal.* **1991**, *128*, 32.

(10) Wang, L. P.; Millman, W. S.; Tysoe, W. T. *Catal. Lett.* **1988**, *1*, 159.

(11) Rucker, T. G.; Logan, M. A.; Gentle, T. M.; Muetterties, E. L.; Somorjai, G. A. *J. Phys. Chem.* **1986**, *90*, 2703.

(12) Wang, L. P.; Tysoe, W. T. *Surf. Sci.* **1990**, *236*, 325.

In addition, the incorporation of a high-pressure reactor into an ultrahigh vacuum apparatus allows the nature of the catalyst surface to be examined following the reaction. This strategy reveals the presence of a rather large thickness (the equivalent of up to  $\sim 10$  monolayers) of a carbon-containing film on the surface during metathesis catalyzed by molybdenum.<sup>19</sup> Similarly stable vinylidene species are formed from acetylene on Pd(111) at  $\sim 300$  K. These do not react to form benzene,<sup>14-18</sup> and the accumulation of this species on the catalyst surface may account for the relatively low activity of palladium as an acetylene trimerization catalyst at high pressure.

Both the rate of olefin metathesis and acetylene cyclotrimerization are accelerated by the addition of hydrogen to the reaction mixture. This is postulated to be due to the titration of these carbonaceous species from the surface. The presence of carbonaceous deposits on the catalyst surface following a catalytic reaction has been observed in other situations, for example, following platinum-catalyzed ethylene hydrogenation.<sup>14</sup> The possible role of these carbonaceous layers during transition-metal-catalyzed hydrocarbon conversion and hydrogenation reactions will also be addressed.

## 2. Experimental Section

A range of equipment was used to carry out these experiments. Ultrahigh vacuum systems generally operated at  $1 \times 10^{-10}$  Torr, and a number of surface-sensitive techniques such as low-energy electron diffraction (LEED), Auger spectroscopy, X-ray and ultraviolet photoelectron spectroscopies (XPS, UPS) and temperature-programmed desorption were used to probe the chemistry of both palladium and molybdenum samples. Of particular importance in examining the catalytic chemistry of model single-crystal samples was the incorporation of an isolatable, high-pressure reactor into the ultrahigh vacuum chamber.<sup>15</sup> The sample was mounted, in this case, onto a coaxial sample manipulator which could be retracted to rest on an anvil. The lower portion of the reactor could be raised to completely enclose the sample, and the seal between the two portions of the cell was made by a copper gasket. This allows the high-pressure cell to operate at pressures up to 1 atm while ultrahigh vacuum ( $2 \times 10^{-10}$  Torr) is maintained in the rest of the apparatus. The cell is filled with gas which is recirculated by means of a pump, and aliquots of the reaction mixture can be diverted to a gas chromatograph or mass spectrometer for analysis. Reaction rates are measured from the concentration of accumulated products as a function of time so that the reaction cell operates as a recirculating batch reactor.

All samples were cleaned using standard protocols, and gases were transferred from the cylinder to a glass bottle for storage. Gases were generally cleaned by bulb-to-bulb distillation prior to use.

## 3. Results and Discussion

**3.1 Acetylene Cyclotrimerization.** Palladium-catalyzed acetylene cyclotrimerization presents an ideal candidate for following a relatively complex reaction pathway in some detail since the benzene formation proceeds both in ultrahigh vacuum<sup>5</sup> and at high pressures.<sup>11</sup> This is illustrated in Figure 1, which displays the 78 amu (benzene) temperature-programmed desorp-

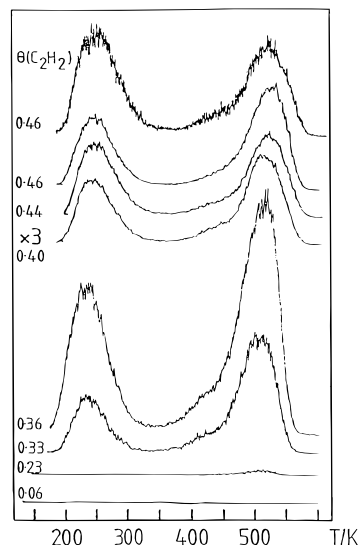


**Figure 1.** Temperature-programmed desorption spectra of benzene (78 amu) obtained following adsorption of acetylene on Pd(111) at 200 K. Acetylene coverage is marked adjacent to the corresponding spectrum.

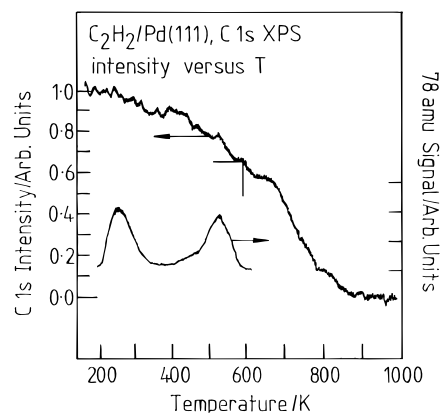


**Figure 2.** Relative surface carbon coverages obtained from the C 1s X-ray photoelectron spectral signal versus temperature after saturating a Pd(111) surface with acetylene at 200 K. Shown for comparison is the corresponding TPD spectrum taken from Figure 1.

tion spectrum following exposure of the surface to various coverages of acetylene.<sup>5</sup> This exhibits an interesting two-peaked structure showing a feature centered at  $\sim 240$  K with a higher temperature state at  $\sim 520$  K. The corresponding acetylene coverage is displayed adjacent to each spectrum. Figure 2 shows a plot of the C 1s X-ray photoelectron spectral intensity measured as a function of annealing temperature following saturation of a Pd(111) surface with acetylene at  $\sim 200$  K.<sup>16</sup> This reveals a continuous diminution in the amount of carbon on the surface as the temperature increases. Shown for comparison is the corresponding TPD spectrum. These results indicate that approximately 30% of the carbon initially present on the surface is removed in this temperature range; roughly this proportion of the acetylene converts to benzene, so that this is a relatively high probability reaction pathway. The catalytic reaction has been studied at high pressures<sup>11</sup> and reveals that Pd(111) catalyzes benzene formation. However, the rate of benzene synthesis is rather insipid in spite of the apparently facile benzene formation found in ultrahigh vacuum, proceeding with a turnover frequency of  $\sim 10^{-2}$  reactions site<sup>-1</sup> s<sup>-1</sup>. The reaction is also catalyzed by alumina-supported palladium.<sup>17</sup> An interesting transient behavior was, however, found in this case. Here, the initial rate of

(13) Bartlett, B.; Soto, C.; Wu, R.; Tysoe, W. T. *Catal. Lett.* **1993**, *21*, 1.

(14) Zaera, F.; Somorjai, G. A. *J. Am. Chem. Soc.* **1984**, *106*, 2288.

(15) Wang, L. P.; Tysoe, W. T. *J. Catal.* **1991**, *128*, 320.

(16) Hoffmann, H.; Zaera, F.; Ormerod, R. M.; Lambert, R. M.; Yao, J. M.; Saldin, D. K.; Wang, L. P.; Bennett, D. W.; Tysoe, W. T. *Surf. Sci.* **1992**, *268*, 1.

(17) Ormerod, R. M.; Lambert, R. M. *J. Chem. Soc., Chem. Commun.* **1990**, *20*, 1421.

(18) Tysoe, W. T.; Nyberg, G. L.; Lambert, R. M. *Surf. Sci.* **1983**, *135*, 128.

(19) Wang, L. P.; Tysoe, W. T.; Ormerod, R. M.; Lambert, R. M.; Hoffmann, H.; Zaera, F.; *J. Phys. Chem.* **1990**, *94*, 4236.

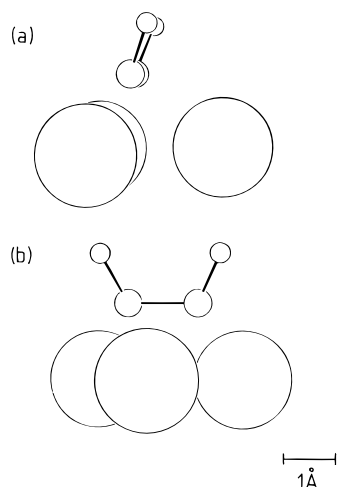


**Figure 3.** Schematic diagram showing the proposed structure of acetylene adsorbed on Pd(111) at 200 K.

benzene formation, immediately after contacting the catalyst surface with acetylene, is found to be extremely high (with initial conversions approaching 100%). The rate, however, decreases monotonically with time on stream to an asymptotic, low steady-state rate which corresponds to the regime in which reactions were carried out on the single-crystal surface. These results raise a number of questions, in addition to the nature of the reaction mechanism. First, benzene appears to be formed in two widely distinct reaction regimes, one at relatively low temperature, and another above room temperature. The origin of these two states will be discussed further below. The second question that will be examined is the possible origin for the decrease in benzene formation rate as a function of time on stream which results in benzene exhibiting such insipid catalytic activity.

The adsorption of acetylene on Pd(111) at around 200 K leads to an overlayer with a saturation coverage of  $\sim 0.46$ .<sup>18</sup> A number of surface-sensitive techniques, including ultraviolet photoelectron spectroscopy<sup>18</sup> and near-edge X-ray absorption fine structure (NEXAFS),<sup>16</sup> as well as theoretical calculations<sup>19,20,21</sup> indicate that this species adsorbs molecularly and is somewhat distorted following adsorption. Figure 3 shows the resulting structure indicating the rehybridization of adsorbed acetylene to  $\sim sp^2$ . A large amount of evidence has accumulated that this reacts with a surface  $C_4$  species to form benzene on the surface. First, the evolution of  $C_4$  is found in molecular beam experiments.<sup>1</sup> Here a continuous beam of acetylene is incident onto the surface and the reaction products are detected mass spectroscopically. Second, the coadsorption of acetylene and hydrogen on the surface yields  $C_4$  products (primarily butene), in addition to ethylene, in thermal desorption spectroscopy.<sup>22</sup> The reaction of acetylene with sulfur<sup>23</sup> or with oxygen<sup>24</sup> yields thiophene and furan, respectively, consistent with the existence on the surface of a stable  $C_4$  species.<sup>25-27</sup> Perhaps the most compelling evidence comes from grafting surface  $C_4$  species onto the

(20) Schneerson, V. L.; Tysoe, W. T.; Saldin, D. K. *Phys. Rev. B*, in press.

(21) Sellars, H. *J. Phys. Chem.* **1990**, *94*, 8329.

(22) Ormerod, R. M.; Lambert, R. M.; Bennett, D. W.; Tysoe, W. T. *Surf. Sci.*, in press.

(23) Gellman, A. *J. Langmuir* **1991**, *7*, 827.

(24) Ormerod, R. M.; Lambert, R. M. *Catal. Lett.* **1990**, *6*, 6971.

(25) Patterson, C. H.; Lambert, R. M. *J. Phys. Chem.* **1983**, *87*, 2469.

(26) Patterson, C. H.; Lambert, R. M. *J. Am. Chem. Soc.* **1988**, *110*, 6871.

(27) Patterson, C. H.; Mundenar, J. M.; Timbrell, P. T.; Gellman, A. J.; Lambert, R. M. *Surf. Sci.* **1989**, *208*, 93.

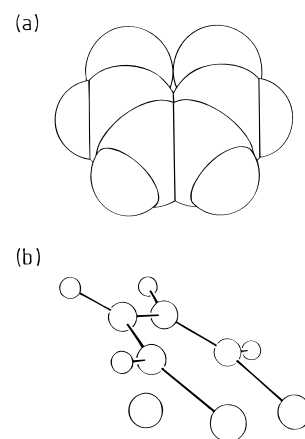


**Figure 4.** Schematic diagram showing the proposed structure of the  $C_4H_4$  species formed by adsorption of  $C_4H_4Cl_2$  on Pd(111) at 90 K and after annealing to 200 K.

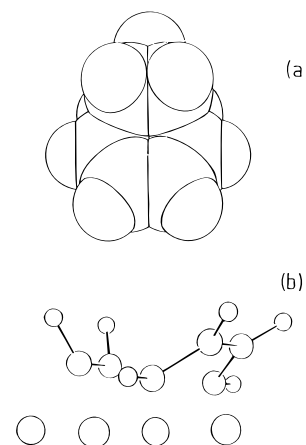


**Figure 5.** Schematic diagram showing the proposed structure of both the  $C_4H_4$  and  $C_2H_2$  species on Pd(111).

surface by thermally decomposing 1,2-dichlorocyclobutene on Pd(111) and subsequently reacting this with acetylene.<sup>25-27</sup> A surface consisting of a mixed overlayer of these two species yields benzene with exactly identical reaction kinetics as when acetylene alone is adsorbed onto the surface, the reaction between the surface  $C_4$  and acetylene being confirmed using isotopic labeling.<sup>27</sup> This latter strategy also allows high concentrations of such surface  $C_4$  species to be prepared and identified.<sup>28</sup> The resulting structure of the surface  $C_4$  species is shown in Figure 4, and this geometry has recently been theoretically confirmed and shown to be thermodynamically stable.<sup>29</sup> The proposed geometry of the surface  $C_2$  and  $C_4$  species engaged in the catalytic act is shown in Figure 5.

Adsorption of acetylene on palladium at  $\sim 300$  K (in contrast to the above experiments where acetylene is adsorbed at  $\sim 200$  K) results in a surface saturation coverage of  $\sim 1.0$ .<sup>18</sup> The nature of the surface species formed at room temperature has also been identified and is depicted in Figure 6. It is proposed to be a vinylidene with its  $C=C$  axis tilted with respect to the surface.<sup>30</sup> Heating a vinylidene-covered surface desorbs *no* benzene so that this is not an active precursor to benzene formation. It is thus likely that the accumulation of this species leads

(28) Ormerod, R. M.; Lambert, R. M.; Hoffmann, H.; Zaera, F.; Yao, J. M.; Saldin, D. K.; Wang, L. P.; Bennett, D. W.; Tysoe, W. T. *Surf. Sci.* **1993**, *295*, 277.

(29) Pacchioni, G.; Lambert, R. M. In press.

(30) Ormerod, R. M.; Lambert, R. M.; Hoffmann, H.; Zaera, F.; Wang, L. P.; Bennett, D. W.; Tysoe, W. T. *J. Phys. Chem.* **1993**, *97*, 3365.

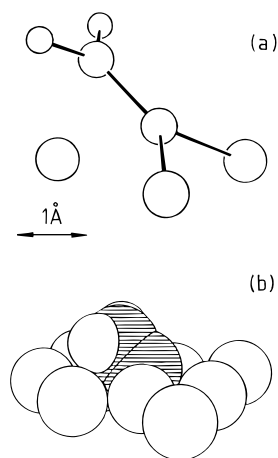


**Figure 6.** Schematic diagram showing the proposed structure of acetylene adsorbed on Pd(111) at 200 K and annealed to  $\sim 300$  K.

to an eventual diminution in the rate of benzene formation found in the transient experiments on supported palladium.

In order to gain insights into the kinetics of benzene formation from acetylene found in TPD, the adsorption of benzene itself on Pd(111) has been studied in detail. Spectroscopic investigations have revealed that the overlayer is oriented with its molecular plane parallel to the Pd(111) surface.<sup>31–42</sup> Temperature-programmed desorption traces (78 amu) found following benzene adsorption are shown in Figure 7.<sup>43</sup> Corresponding benzene coverages are marked adjacent to each spectrum. Note that *no* benzene is found to desorb for coverages less than 0.05 monolayers; benzene completely thermally decomposes to desorb hydrogen and deposit carbon onto the surface. At larger coverages, there is a precipitate switch in the observed chemistry and any additional benzene adsorbed onto the surface desorbs molecularly without any decomposition. This benzene desorbs in a state centered at 520 K, coincident with the high-temperature state found following adsorption of acetylene. This result is consistent with the postulate that benzene formation is desorption-rate limited in this state. The spectra have been explained using Monte Carlo calculations.<sup>43,44</sup>

The desorption spectra in Figure 8 show the effect of extremely large subsequent benzene exposures to Pd(111); this results in the growth of a peak centered at  $\sim 260$  K. Note that this temperature is identical to that of the low-temperature benzene desorption state found following

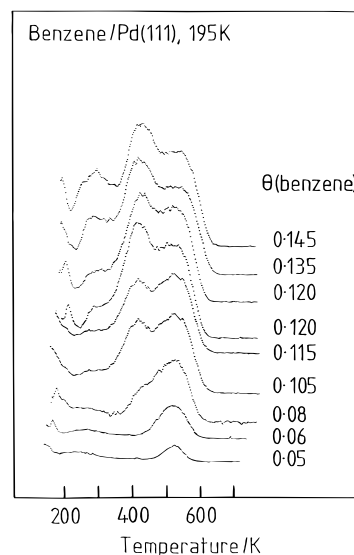


**Figure 7.** Temperature-programmed desorption spectra of benzene (78 amu) obtained following adsorption of benzene on Pd(111) at 200 K. Benzene coverage is marked adjacent to the corresponding spectrum.

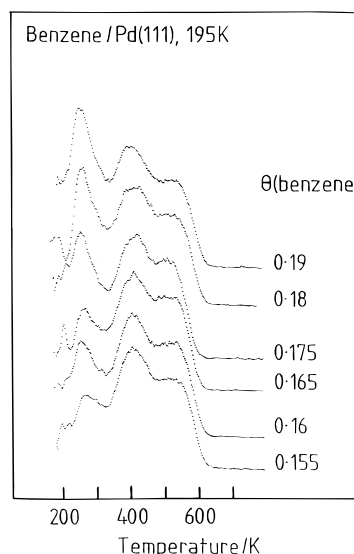


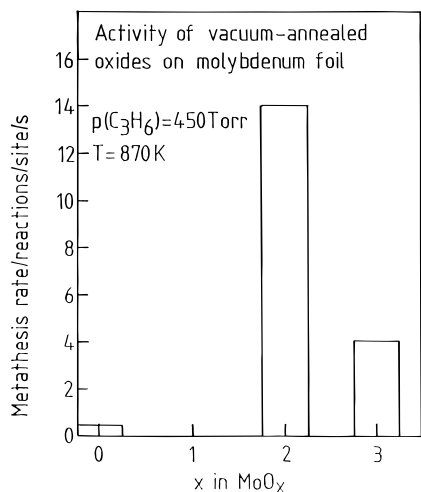
**Figure 8.** Temperature-programmed desorption spectra of benzene (78 amu) obtained following adsorption of benzene on Pd(111) at 200 K using high exposures. Benzene coverage is marked adjacent to the corresponding spectrum.

acetylene adsorption. This state is assigned to the formation of *tilted* benzene that is induced by additional benzene that is accommodated onto the surface. There are several pieces of evidence for this proposal. First, this state is not due to the condensation of multilayers since these have been seen and the resulting desorption state is at a significantly lower temperature ( $\sim 150$  K).<sup>45</sup> Second, NEXAFS shows the presence of tilted benzene<sup>43</sup> at high coverages ( $\sim 0.22$ ).<sup>46</sup> Finally, the sticking probability onto this state is very low ( $\sim 3\%$ ), certainly much less than would be expected for multilayer condensation.

In summary, benzene is therefore formed on Pd(111) via the rapid interaction of adsorbed acetylene and a surface  $C_4$  metallocycle. The resulting benzene is sterically crowded and adopts a tilted configuration desorbing

- (31) Netzer, F. P.; Mach, J. U. *J. Chem. Phys.* **1983**, *79*, 1017.  
 (32) Wadill, G. D.; Kesmodel, L. L. *Phys. Rev. B* **1985**, *31*, 4940.  
 (33) Huber, W.; Steinruck, H. P.; Pache, T.; Menzel, D. *Surf. Sci.* **1989**, *217*, 103.  
 (34) Huber, W.; Zebisch, P.; Bornemann, T.; Steinruck, H. P. *Surf. Sci.* **1991**, *258*, 16.  
 (35) Johnson, A. L.; Muetterties, E. L.; Stöhr, J. *J. Am. Chem. Soc.* **1983**, *105*, 7183.  
 (36) Somers, J.; Bridge, M. E.; Lloyd, D. R.; McCabe, T. *Surf. Sci.* **1987**, *181*, L167.  
 (37) Ogletree, D. F.; Van Hove, M. A.; Somorjai, G. A. *Surf. Sci.* **1987**, *183*, 183.  
 (38) This footnote was deleted in revision.  
 (39) Van Hove, M. A.; Lin, R.; Somorjai, G. A. *Phys. Rev. Lett.* **1983**, *51*, 778.  
 (40) Koel, B. A.; Crowell, J. E.; Mate, C. M.; Somorjai, G. A. *J. Phys. Chem.* **1984**, *88*, 1988.  
 (41) Neumann, M.; Mack, J. U.; Bertell, E.; Netzer, F. P. *Surf. Sci.* **1987**, *155*, 629.  
 (42) Netzer, F. P.; Rosina, G.; Bertel, E.; Saalfeld, H. *Surf. Sci.* **1987**, *184*, L397.  
 (43) Tysøe, W. T.; Ormerod, R. M.; Lambert, R. M.; Zgrablich, G.; Ramirez-Cuesta, H. *J. Phys. Chem.* **1993**, *97*, 3365.  
 (44) Sales, J. L.; Zgrablich, G. *Surf. Sci.* **1987**, *187*, 1.

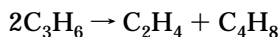
- (45) Patterson, C. H.; Lambert, R. M. *J. Phys. Chem.* **1988**, *92*, 1266.  
 (46) Hoffmann, H.; Zaera, F.; Ormerod, R. M.; Lambert, R. M.; Wang, L. P.; Tysøe, W. T. *Surf. Sci.* **1990**, *232*, 259.



**Figure 9.** Histogram showing the relative metathesis activities for model catalysts consisting of Mo, MoO<sub>2</sub>, and MoO<sub>3</sub> for reaction at 870 K using 450 Torr of propylene.

in a state centered at  $\sim 260$  K. As the desorption sweep proceeds, the surface crowding is relieved, allowing any remaining benzene to lie flat on the surface and to desorb from this state at  $\sim 520$  K. In addition, adsorbed acetylene converts to a more thermodynamically stable vinylidene species above  $\sim 300$  K. The accumulation of this species may be responsible for the low steady-state rate of benzene formation by Pd(111) model catalysts at higher pressures.

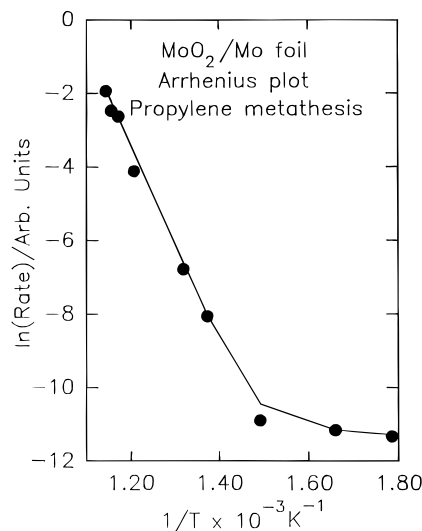
**3.2 Olefin Metathesis.** The olefin metathesis reaction was discovered by Banks and Bailey and is catalyzed in both homogeneous and heterogeneous phases.<sup>47-51</sup> Heterogeneous catalysts for this reaction are generally supported oxides of molybdenum, rhenium, or tungsten. The simplest example of this reaction is the metathesis of propylene:



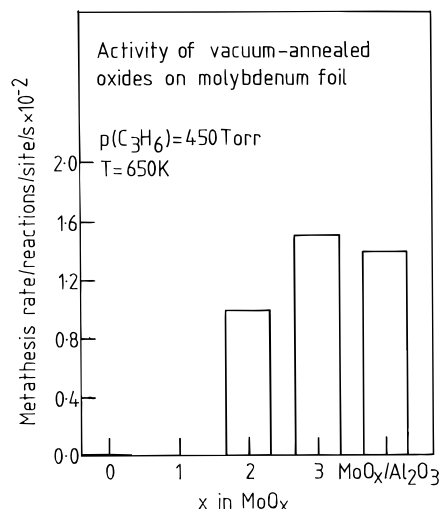
In order to establish which oxidation states of molybdenum provide the most effective catalysts for this reaction, a series of model systems, metallic molybdenum, MoO<sub>2</sub>, and MoO<sub>3</sub>, were prepared and their catalytic activities measured.<sup>52</sup> MoO<sub>2</sub> was synthesized by controlled oxidation of metallic molybdenum in the ultrahigh vacuum portion of the apparatus and characterized using Auger, X-ray, and ultraviolet photoelectron spectroscopies and by low-energy electron diffraction. MoO<sub>3</sub> was made by oxidation of metallic molybdenum at high pressures using the high-pressure reactor.

Figure 9 shows a histogram of the relative activity for olefin metathesis of the three model systems at a relatively high reaction temperature (870 K), and clearly, MoO<sub>2</sub> provides the most, and metallic molybdenum the least, effective catalyst.

Figure 10 displays the temperature dependence of propylene metathesis catalyzed by the most active catalyst, MoO<sub>2</sub>, plotted in Arrhenius form. This shows two distinct regimes: one above  $\sim 650$  K where the reaction activation energy is  $\sim 60$  kcal/mol, and another below this temperature, where the activation energy is  $\sim 6$  kcal/mol. The



**Figure 10.** Arrhenius plot for olefin metathesis catalyzed by an MoO<sub>2</sub> model catalyst.



**Figure 11.** Histogram showing the relative metathesis activities for model catalysts consisting of Mo, MoO<sub>2</sub>, and MoO<sub>3</sub> for reaction at 650 K using 450 Torr of propylene. Shown for comparison is the reaction rate for a high loading (18.6%) of alumina-supported molybdena.<sup>47</sup>

pressure dependence in the high-temperature regime is first order in propylene pressure. This result suggests that there are two distinct reaction regimes depending on the temperature.

The corresponding relative activities for the model catalysts, Mo, MoO<sub>2</sub>, and MoO<sub>3</sub>, have been measured in a similar way for reaction in the low-temperature regime, that is, for olefin metathesis catalyzed at 650 K. The results are shown plotted in histogram form in Figure 11. Note the lower reaction rates reflecting the lower reaction temperature. MoO<sub>3</sub> now forms the most effective catalyst, MoO<sub>2</sub> still displays significant activity, and metallic molybdenum is essentially inactive (consistent with the high activation energy for this catalyst). Also plotted onto these data is the activity measured for an alumina-supported MoO<sub>x</sub> catalyst with a high molybdenum oxide loading (18.6%), which agrees well with the rates measured for the model oxides.<sup>47</sup> In addition, the activation energy measured for this reaction ( $\sim 6$  kcal/mol) is within the range of those measured for metathesis catalysts and suggests that an oxide grown on a molybdenum substrate provides a good model for a high-loading, supported catalyst.

(47) Thomas, R.; Moulijn, J. A. *J. Mol. Catal.* **1982**, *15*, 157.

(48) Rooney, J. J.; Stewart, A. *Catalysis* **1977**, *1*, 277.

(49) Brenner, A.; Burwell, R. L., Jr. *J. Catal.* **1978**, *52*, 364.

(50) Abdo, S.; LoJacono, M.; Clarkson, R. B.; Hall, W. K. *J. Catal.* **1975**, *36*, 330.

(51) Millman, W. S.; Crespin, M.; Cirrillo, A. L.; Abdo, S.; Hall, W. K. *J. Catal.* **1979**, *60*, 404.

(52) Bartlett, B.; Soto, C.; Wu, R.; Tysoe, W. T. *Catal. Lett.* **1993**, *21*, 1.

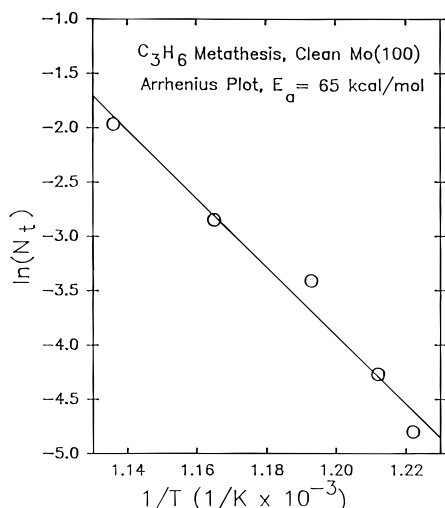


**Figure 12.** Arrhenius plot for olefin metathesis catalyzed by a Mo(100) single crystal model.

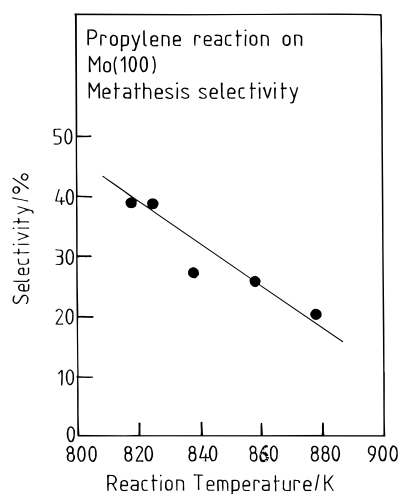


**Figure 13.** Selectivity to olefin metathesis catalyzed by Mo(100) plotted versus reaction temperature.

Figure 12 shows the corresponding Arrhenius plot for reaction catalyzed by metallic molybdenum (the worst catalyst),<sup>3</sup> which is capable of catalyzing the reaction at sufficiently high temperature. The activation energy in this case is ~65 kcal/mol, very similar to that found for MoO<sub>2</sub> at high temperature. These results suggest that the reaction pathway at high temperatures is similar for both catalysts. In addition to the formation of metathesis products, a significant rate of alkene hydrogenolysis is found. Shown in Figure 13 is the metathesis selectivity of clean metallic molybdenum, the remaining products being due to hydrogenolysis.

The commonly accepted mechanism for olefin metathesis holds that reaction is initiated by the formation of carbenes that provide the catalytically "active site". This is proposed to react with an alkene to form a surface metalocycle which decomposes via the reverse of this reaction to yield products.<sup>53-57</sup> However, the carbene-metalocycle mechanism has been suggested for catalysts only at low temperatures (<650 K), and this suggests that

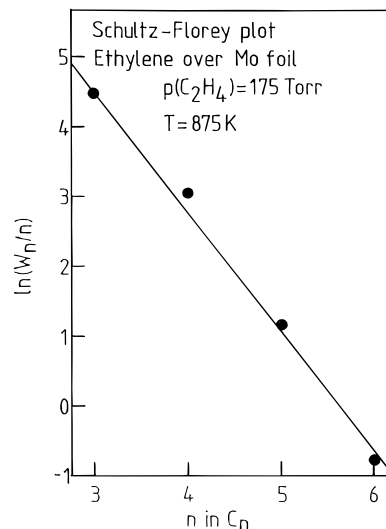
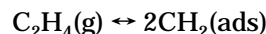


**Figure 14.** A Schulz-Florey plot of the distribution of hydrocarbons formed in the reaction of ethylene catalyzed by Mo(100) at 875 K using 175 Torr of ethylene.

there may be another mechanism that predominates at higher temperatures. We have therefore studied the reaction of ethylene catalyzed by metallic molybdenum.<sup>58</sup> In this case, olefin metathesis is degenerate in the sense that metathesis of ethylene merely yields ethylene. However, careful examination of the reaction products reveals the formation of higher hydrocarbons. Shown plotted in Figure 14 is the product distribution resulting from reaction of ethylene catalyzed by metallic molybdenum plotted in Schulz-Florey form (by plotting  $\ln(W_n/n)$  versus  $n$ , where  $W_n$  is the yield of a hydrocarbon with  $n$  carbons).<sup>58</sup> This yields a good straight line, which indicates that the higher hydrocarbons are formed by the polymerization of C<sub>1</sub> monomers. This reaction is similar to the surface polymerization step on Fischer-Tropsch synthesis, and it has been shown previously that metallic molybdenum can catalyze hydrocarbon formation from the reaction of CO and H<sub>2</sub>.<sup>59</sup> This indicates that metathesis could occur by a simple recombination reaction of dissociated hydrocarbon fragments as



This suggests that olefin metathesis proceeds, above ~650 K, not by the conventionally proposed carbene-metalocycle mechanism but rather by a dissociative-associative pathway. This route has also been suggested for the removal of carbene "active sites" during metathesis at lower temperatures.

In order to establish whether reaction products formed in the high-temperature metathesis of propylene are consistent with such a mechanism, the Schulz-Florey mechanism can be modified to calculate the product distribution arising from propylene dissociation products, and this yields<sup>58</sup>

$$W_n = (kp^{n-1}/\alpha)((1 + \alpha)^{n+1} - (1 - \alpha)^{n+1})$$

where  $\alpha = (1 + (8/p))^{1/2}$  and  $p$  and  $k$  are constants, where  $p$  corresponds to the propagation probability for growth of the polymer and  $k$  is a normalization constant. This is plotted in histogram form and compared with the

(58) Bartlett, B. F.; Schneerson, V. L.; Tysoe, W. T. *Catal. Lett.* In press.

(59) Logan, M.; Gellman, A. J.; Somorjai, G. A. *J. Catal.* **1980**, *63*, 226.

(53) Hérrison, J. L.; Chauvin, Y. *Makromol. Chem.* **1970**, *141*, 161.

(54) Carden, D. J.; Doyle, M. J.; Lappert, M. F. *J. Chem. Soc., Chem. Commun.* **1972**, 927.

(55) Ephritikhine, M.; Green, M. L. H.; MacKenzie, R. E. *J. Chem. Soc., Chem. Commun.* **1976**, 619.

(56) Kazuta, M.; Tanaka, K. *Catal. Lett.* **1988**, *7*.

(57) Vikulov, K. A.; Elev, I. V.; Shelomov, B. N.; Kazansky, V. B. *Catal. Lett.* **1989**, *2*, 121.

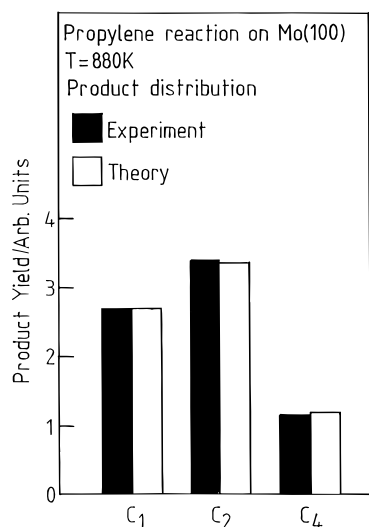


**Figure 15.** Histogram comparing the product distribution for the reaction of propylene catalyzed by Mo(100) at 880 K (filled bars) with a theoretical prediction (open bars); see text.

experimental product distribution in Figure 15. Clearly the agreement between experiment and theory is good. Similarly good agreement can be obtained for product distributions from reaction under various conditions and is consistent with the proposal that olefin metathesis proceeds via an alkene dissociation–association mechanism at high temperatures.

The study of the surface chemistry of alkenes on metallic molybdenum shows that they are considerably distorted following adsorption at low temperature.<sup>60–62</sup> Photoelectron spectroscopy can be used to probe the shallow 2s-derived molecular orbitals and has proven very useful in following chemical changes on these surfaces. It has been demonstrated that the gas-phase photoemission spectra of the 2s-derived molecular orbital region can be described extremely well using simple Hückel theory.<sup>63–65</sup> Such a simple quantitative calculation is not possible for adsorbed molecules because of other initial- and final-state effects. Nevertheless, the patterns of the peaks due to the 2s-derived molecular orbital can be used to establish the nature of the hydrocarbon on the surface.<sup>66</sup> This is illustrated in Figure 16, which displays photoelectron spectra, taken using 80 eV photons, for a range of molecules adsorbed at low temperature on a molybdenum surface. The peak positions agree well with predictions from a simple molecular orbital analysis. The corresponding spectrum obtained following ethylene adsorption at low temperature displays two peaks due to emission from the C(2s) + C(2s) bonding and the C(2s) – C(2s) antibonding orbitals. On warming the surface to room temperature, only a single peak is present, indicating the formation of a surface C<sub>1</sub> species.<sup>59</sup> This indicates rapid carbon–carbon bond dissociation for ethylene on Mo(100), a result that is consistent with the associative–dissociative mechanism outlined above.

Analysis of the surface following reaction catalyzed by Mo(100) reveals the presence of a large amount of surface

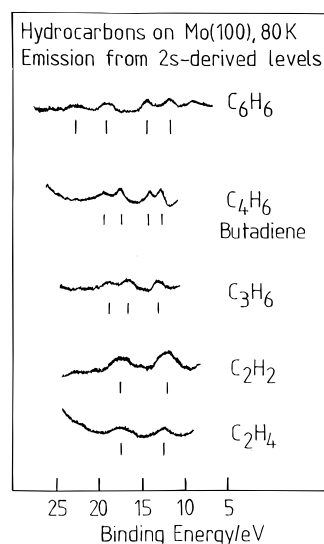


**Figure 16.** Photoelectron spectra of the C 2s-orbital derived region for various molecules adsorbed on Mo(100) at 80 K taken using 80 eV photons.

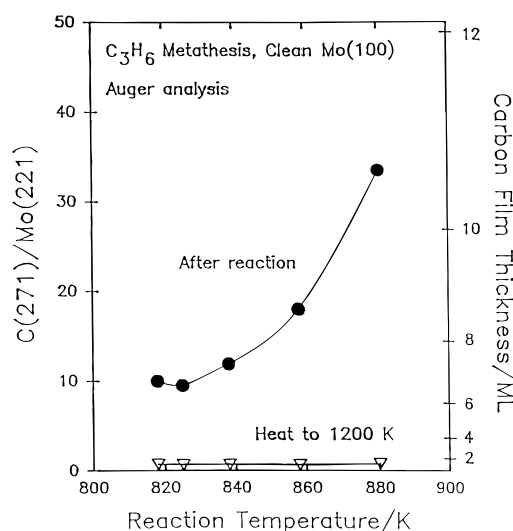


**Figure 17.** Plot of the carbon/molybdenum Auger intensity ratio (C(271)/Mo(221)) found on a Mo(100) surface following propylene metathesis. The reaction temperature is marked on the abscissa. Plotted also is the estimated carbon film thickness.

carbon.<sup>9</sup> Shown in Figure 17 is a plot of the C/Mo Auger ratio obtained for the catalyst surface following reaction at various temperatures. The approximate film thickness can be estimated using the Auger escape depth, and these values are also indicated on the graph. It is clear that the equivalent of several monolayers of carbon are present on the surface. In order to establish whether this affects the catalytic activity, the following “restart” reaction was carried out. The rate of olefin metathesis was measured for a clean sample, and the resulting product accumulation curve is displayed in Figure 18 (●). The sample was then removed from the high-pressure reactor, and the presence of a substantial amount of carbon was confirmed using Auger spectroscopy. The sample was then reinserted into the high-pressure reactor and the reaction started once again using exactly identical reaction conditions. As shown by the data in Figure 18 (○), products accumulate at exactly the same rate on the carbon-covered surface as on the initially clean sample; reaction can proceed in the presence of substantial amounts of carbon on the surface. Temperature-programmed desorption of the catalyst following reaction evolves both hydrogen and hydrocarbon

(60) Wang, L. P.; Tysoe, W. T. *Surf. Sci.* **1990**, *230*, 74.

(61) Wang, L. P.; Tysoe, W. T. *Surf. Sci.* **1990**, *236*, 325.

(62) Wang, L. P.; Tysoe, W. T. *Surf. Sci.* **1991**, *245*, 41.

(63) Potts, A. W.; Williams, T. A.; Price, W. C. *Faraday Discuss. Chem. Soc.* **1972**, *54*, 104.

(64) Potts, A. W.; Streets, D. G. *J. Chem. Soc., Faraday Trans. 2* **1974**, *2*, 875.

(65) Streets, D. G.; Potts, A. W. *J. Chem. Soc., Faraday Trans. 2* **1974**, *2*, 1505.

(66) Wang, L. P.; Hinkelman, R.; Tysoe, W. T. *J. Electron Spectrosc. Relat. Phenom.* **1991**, *56*, 341.

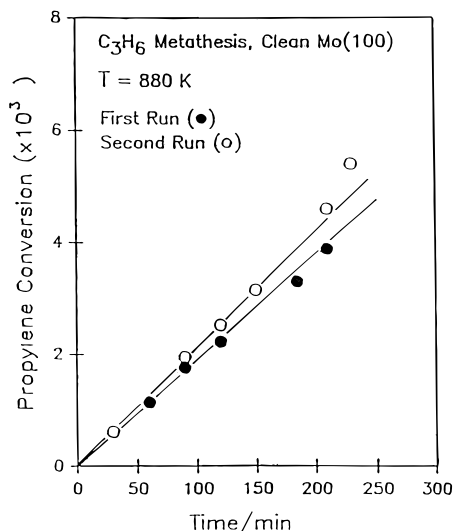


**Figure 18.** Product accumulation curve for propylene metathesis catalyzed by Mo(100) at 880 K. Filled circles show data for the initially clean Mo(100) sample, and open circles, data for the sample after initial reaction following removal into ultrahigh vacuum and reinsertion into the high-pressure reactor.

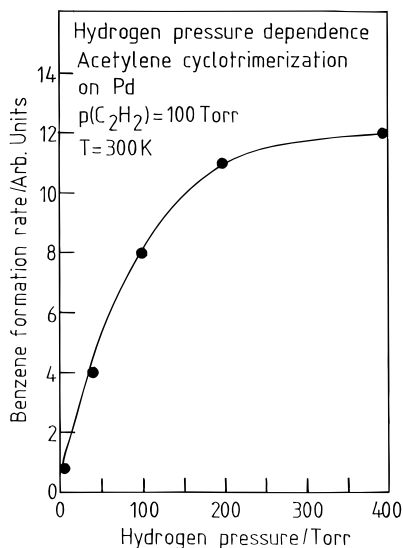


**Figure 19.** Plot showing the effect of the addition of hydrogen on the rate of formation of benzene from acetylene catalyzed by palladium for reaction at 300 K using 100 Torr of acetylene.

fragments.<sup>9</sup> The nature of the surface species is currently being investigated using infrared spectroscopy.

**3.3 Effect of Hydrogen on Hydrocarbon Conversion Catalysis.** A common feature of the hydrocarbon reactions discussed here is the presence of a stable carbonaceous layer during reaction. In the case of olefin metathesis, this consists of a thick layer, and in the case of acetylene cyclotrimerization, it is a vinylidene monolayer. It has also been shown that platinum-catalyzed ethylene hydrogenation proceeds in the presence of a monolayer of ethylidyne which is *not* the precursor to ethane formation. An elegant series of experiments using <sup>14</sup>C-labeled ethylene show that the ethylidyne layer can be removed using high pressures (~1 atm) of hydrogen.<sup>14</sup> The effect of hydrogen on both acetylene cyclotrimerization and olefin metathesis, reactions that themselves do not involve hydrogen as a reactant, was therefore investigated. The result of such an experiment for acetylene cyclotrimerization is shown in Figure 19. Here the rate of benzene formation is plotted *versus* pressure of hydrogen for

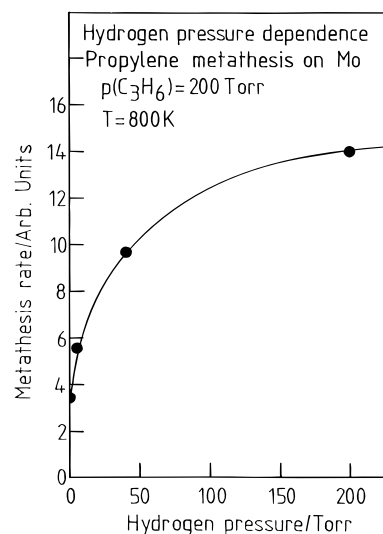


**Figure 20.** Plot showing the effect of the addition of hydrogen on the rate of propylene metathesis catalyzed by molybdenum for reaction at 800 K using 200 Torr of propylene.

reaction at 300 K. Benzene formation, in the absence of hydrogen, is extremely low at this temperature,<sup>11</sup> but the addition of hydrogen results in a significant increase in the benzene formation rate. Preliminary experiments using deuterium rather than hydrogen suggest that no deuterium is incorporated into the product benzene for reaction at 300 K, suggesting that no new reaction pathway is being opened up that involved reaction with hydrogen.

A similar effect is found for the metathesis of propylene (Figure 20), another reaction that proceeds in the presence of a carbonaceous layer but does not involve hydrogen directly. It should be noted that conventional hydrogenation products, consisting of ethylene and butene in the case of the palladium-catalyzed reaction of acetylene, and propane in the case of molybdenum-catalyzed reaction of propylene, are also found. Since reactants are being titrated from the surface, this should result in a *diminution* in reaction rate rather than an enhancement. In view of the results presented above, it is proposed that the effect of the added hydrogen is to remove strongly bound carbonaceous deposits from the surface to reveal the active, bare metal sites below.

A similar effect is therefore *also* likely to operate in reactions that *do* involve hydrogen, for example, ethylene hydrogenation. The high-pressure reaction kinetics for Pt(111)-catalyzed ethylene hydrogenation have been measured in detail.<sup>14</sup> In addition, it is found that coadsorption of ethylene and hydrogen on Pt(111) *in vacuo* yields ethane, allowing the kinetic parameters for this process to be calculated.<sup>67</sup> Using these parameters, a model for ethylene hydrogenation, depicted in Figure 21a, is analyzed to yield the corresponding steady-state rate, and the resulting prediction is compared with the calculated rate as a function of reaction temperature, plotted in Arrhenius form, in Figure 22. Clearly, the predicted reaction rate is substantially larger than that found experimentally. Such a disparity between the calculated and the experimental rate has also been noted previously.<sup>67</sup> As mentioned above, it has been shown that the reaction proceeds in the presence of a saturated ethylidyne layer, and in this case, it has been shown that, although ethylidyne *are* titrated from the surface by a high pressure of hydrogen, this rate is far too low to account for the catalytic rate of ethane formation. In view of the results

(67) Godbey, D.; Zaera, F.; Yeates, R.; Somorjai, G. A. *Surf. Sci.* **1986**, *167*, 166.



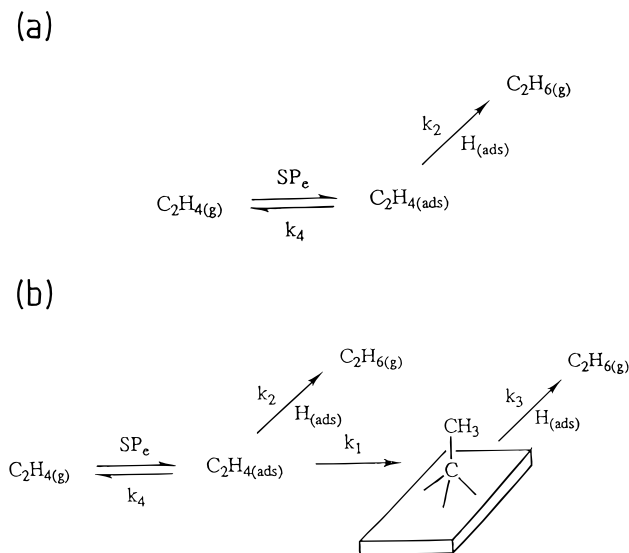


**Figure 21.** (a) Model for the reaction of ethylene with hydrogen to form ethane catalyzed by Pt(111) and (b) the same reaction scheme showing the formation and removal of surface ethyldynes.

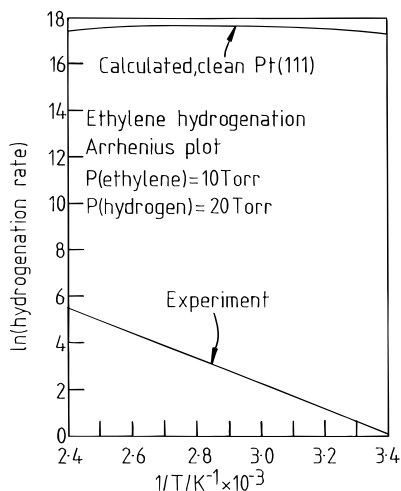


**Figure 22.** Comparison of the Pt(111)-catalyzed ethylene hydrogenation rate calculated for the model shown in Figure 21a compared with experimental results.

presented above, which suggest that hydrogen can react with strongly bound surface carbonaceous species to reveal the active metal sites below, a similar phenomenon is proposed to operate in this case. That is, hydrogen is proposed to play two roles in ethylene hydrogenation. First, it acts as a reactant to produce ethane, and, second, it acts also as a "surface cleaner" to remove carbonaceous species from the catalyst. The reaction scheme adopted, in this case, is shown in Figure 21b, which now includes both ethyldyne formation and rehydrogenation. Note that there are precedents for all of the reaction steps indicated in Figure 21b in the surface science literature. A simple steady-state analysis of this model shows that the rate of hydrogenation  $r_{\text{H}}$  is given by

$$r_{\text{H}} = (k_2 k_3 / k_1) p(\text{H}_2)^{1.5}$$

and is zero order in ethylene pressure. Hydrogen is assumed to be in equilibrium with the surface. A hydrogen pressure dependence greater than unity arises naturally from the notion that hydrogen is performing a dual role: hydrogenating ethylene to form ethane and removing ethyldyne to provide vacant surface sites. That is, the

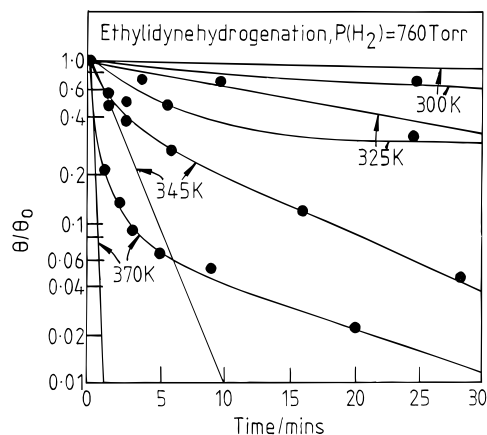


**Figure 23.** Plot of the ethyldyne coverage on Pt(111) as a function of time for reaction with 1 atm of hydrogen at various temperatures (●) compared with values calculated from the experimental ethylene hydrogenation rates using the scheme depicted in Figure 21b.

"active-site" density, where active sites are just vacant metal sites, depends on the hydrogen pressure. The rate constants  $k_1$  and  $k_2$  have been established for the clean surface using temperature-programmed desorption.<sup>67</sup> The rate constant  $k_3$  can, in principle, be determined from a plot of  $\ln(\Theta(\text{ethyldyne}))$  versus time for ethyldyne rehydrogenation (Figure 23<sup>14</sup>). Experimentally, however, this graph is found not to be linear throughout the whole range. Part of this effect is likely to be due to surface contamination arising from the long exposure times and repeated insertions into the high-pressure reactor required to collect these data. Instead, the value of  $k_3$  that yields the best agreement with the catalytic rate on Pt(111) has been measured and yields a value of  $0.55 \exp(-26800/RT)$ . The rate of ethyldyne rehydrogenation required by both the model and catalytic results is shown in Figure 23, which plots the relative ethyldyne coverage versus time in a semilogarithmic plot as straight lines. Plotted also on this curve are the experimental results (●) for the rate of ethyldyne rehydrogenation taken from the data of ref 14, and the two values are in reasonable agreement. Note also that the value of  $k_3$  is substantially lower than the rate of hydrogen desorption from Pt(111), indicating that this species is not effectively rehydrogenated by coadsorbed hydrogen in TPD as found experimentally. Finally, the ethyldyne coverage predicted by this model is always in excess of 99% of saturation under the conditions used for ethylene hydrogenation, and  $1 - \Theta(\text{ethyldyne})$  is shown plotted versus reaction temperature in Figure 24 for the conditions 10 Torr of ethylene and 20 Torr of hydrogen. These results are consistent with the detection of an ordered LEED pattern on the Pt(111) surface after reaction, implying the continued existence of an almost saturated surface while catalysis proceeds.

More precise analysis of both TPD results and the steady-state catalytic reaction using more recent kinetic measurements<sup>68,69</sup> and more detailed Monte Carlo simulations will also help in linking surface science kinetic measurements with high-pressure, steady-state catalytic reactions via models such as the ones proposed here.

#### 4. Conclusions

Palladium-catalyzed acetylene cyclotrimerization proceeds via a rapid surface reaction between adsorbed acetylene and a surface  $\text{C}_4$  metallocycle. The accumulation

(68) Zaera, F. *J. Phys. Chem.* **1990**, *94*, 5090.

(69) Zaera, F. *J. Phys. Chem.* **1990**, *94*, 8350.

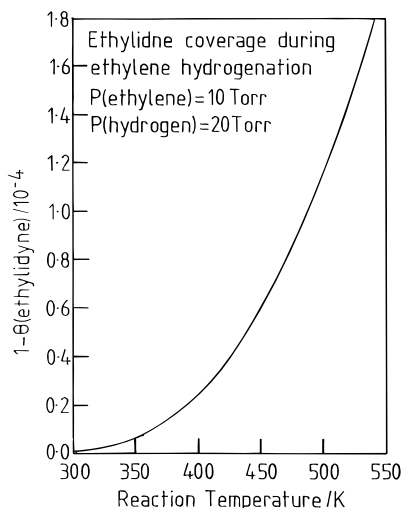


**Figure 24.** Plot showing the calculated value of  $1 - \Theta$  (ethylidyne) versus reaction temperature during Pt(111)-catalyzed ethylene hydrogenation using 10 Torr of ethylene and 20 Torr of hydrogen.

of vinylidene species on the surface is proposed to be responsible for the low catalytic activity at high pressures.

It is also shown that the most effective olefin metathesis catalyst consists of  $\text{MoO}_2$  or  $\text{MoO}_3$ , and two reaction regimes are found for this reaction: one below 650 K, which resembles high loadings of supported molybdenum oxide, and a region above this temperature, which proceeds with a high reaction activation energy ( $\sim 60$  kcal/mol). It

is suggested that metathesis proceeds, in this case, via an associative mechanism.

Both hydrocarbon conversion reactions proceed in the presence of a carbonaceous layer. In the case of acetylene cyclotrimerization, this is suggested to consist of a vinylidene layer, and for olefin metathesis, it is a thick carbonaceous film. The rates of both reactions are substantially increased by the addition of hydrogen to the reaction mixture, even though the reactions themselves do not involve hydrogen. This effect is ascribed to the removal of the carbonaceous layer from the surface during reaction to reveal vacant metal sites below. Application of these ideas to Pt(111)-catalyzed ethylene hydrogenation effectively rationalizes the observed reaction kinetics and shows that the best agreement between the calculated and experimental rates is found when reaction occurs on a surface that is *almost* fully saturated with an ethylidyne layer. In this case, it is proposed that hydrogen can perform a dual role. First, it acts as a reactant to form ethane, and second, it acts as a "cleaner" to remove strongly bound carbonaceous species from the surface to reveal vacant catalytic sites below.

**Acknowledgment.** We gratefully acknowledge support of this work by the U.S. Department of Energy, Division of Chemical Sciences, Office of Basic Energy Sciences, under Grant No. FG02-92ER14289 and to the donors of the Petroleum Research Fund, administered by the American Chemical Society.

LA9406970